EARTH SURFACE PROCESSES AND LANDFORMS
Earth Surf. Process. Landforms (2013)

Published online in Wiley Online Library
(wileyonlinelibrary.com) DOI: 10.1002/esp.3491

Modeling the effects of pulsed versus chronic sand inputs on salmonid spawning habitat in a low-gradient gravel-bed river

Oscar Maturana,[1]* Daniele Tonina,[2] James A. McKean,[3] John M. Buffington,[3] Charles H. Luce[3] and Diego Caamaño[4]
[1] Departamento de Ingeniería Civil, Universidad de Concepción, Barrio Universitario S/N, Concepción, Chile
[2] Center for Ecohydraulics Research, University of Idaho, College of Engineering-Boise, 322 E. Front St, Ste. 340, Boise, ID 83702
[3] US Forest Service, Rocky Mountain Research Station, 322 E. Front St, Ste. 401, Boise, ID 83702
[4] Departamento de Ingeniería Civil, Universidad Católica de la Santísima Concepción, Alonso de Ribera 2850, Concepción, Chile

Received 10 January 2013; Revised 27 September 2013; Accepted 30 September 2013

*Correspondence to: O. Maturana, Departamento de Ingeniería Civil, Universidad de Concepción, Barrio Universitario S/N, Concepción, Chile.
E-mail: oscar.maturana.g@gmail.com

ESPL
Earth Surface Processes and Landforms

ABSTRACT: It is widely recognized that high supplies of fine sediment, largely sand, can negatively impact the aquatic habitat quality of gravel-bed rivers, but effects of the style of input (chronic vs. pulsed) have not been examined quantitatively. We hypothesize that a continuous (i.e. chronic) supply of sand will be more detrimental to the quality of aquatic habitat than an instantaneous sand pulse equal to the integrated volume of the chronic supply. We investigate this issue by applying a two-dimensional numerical model to a 1 km long reach of prime salmonid spawning habitat in central Idaho. Results show that in both supply scenarios, sand moves through the study reach as bed load, and that both the movement and depth of sand on the streambed mirrors the hydrograph of this snowmelt-dominated river. Predictions indicate greater and more persistent mortality of salmonid embryos under chronic supplies than pulse inputs, supporting our hypothesis. However, predicted mortality varies both with salmonid species and location of spawning. We found that the greatest impacts occur closer to the location of the sand input under both supply scenarios. Results also suggest that reach-scale morphology may modulate the impact of sand loads, and that under conditions of high sand loading climate-related increases in flow magnitude could increase embryo mortality through sand deposition, rather than streambed scour.

KEYWORDS: sediment transport; pulsed and chronic sand supply; aquatic habitat; river morphology; gravel-bed rivers

Introduction

The magnitude, frequency, and caliber of sediment supply affect river morphology and the availability and quality of aquatic habitats. In particular, high supplies of fine sediment (< 6 mm) can have detrimental effects on salmonid spawning habitat (Everest *et al.*, 1987; Chapman, 1988; Bjornn and Reiser, 1991; Cover *et al.*, 2008). Salmonids incubate their young within nests (redds) constructed in streambed gravels and cobbles (Burner, 1951). However, high supplies of fine sediment can clog pore spaces in redds and reduce the hyporheic flow of dissolved oxygen to incubating embryos (Everest *et al.*, 1987; Lapointe *et al.*, 2004; Grieg *et al.*, 2005; Tonina and Buffington, 2009). Furthermore, it can physically entomb embryos, inhibiting their emergence from the streambed (Everest *et al.*, 1987; Bjornn and Reiser, 1991; Rhodes *et al.*, 1994; May *et al.*, 2009). Fine sediment can also reduce the growth and survival of juvenile salmonids foraging on the streambed (Bjornn *et al.*, 1977; Suttle *et al.*, 2004). Consequently, fine sediment input from land management activities, such as road construction, forest harvest, and prescribed burning is a concern in salmon-bearing streams. Although there are clear physical mechanisms by which fine sediment affects reproductive success in salmonids, the relationship between fine sediment inputs and fish stocks and recruitment in natural systems remains uncertain (Everest *et al.*, 1987; Cover *et al.*, 2008). The reason is that sediment (broadly defined) has positive and negative roles in aquatic ecology. Sediment is the habitat in one sense, and the coarse sediments that are necessary for spawning (gravel and cobble) commonly enter the stream accompanied by detrimental fine sediments (Everest *et al.*, 1987; Reeves *et al.*, 1995). However, fine sediment also carries with it nutrients that are important for aquatic productivity (Wood and Armitage, 1997).

This duality becomes important in the context of the debate about management of fire and fuels in forestlands and understanding the tradeoffs between wildfires and land management options available to mitigate their extent and severity (Bisson *et al.*, 2003; Riemann *et al.*, 2010). Wildfires are associated with extreme inputs of sediment to streams (Istanbulluoglu *et al.*, 2002; Miller *et al.*, 2003; Hoffman and Gabet, 2006; Shakesby and Doerr, 2006; Moody and Martin, 2009; Cannon *et al.*, 2010), but with relatively long recurrence periods between events. However, the effect of land management on long-term sediment yields is expected to be small because of the controls imposed by soil generation and diffusive hillslope transport processes (Istanbulluoglu *et al.*, 2004), and because most anthropogenic sediment inputs (e.g., forest roads) are minor relative to long-term natural sediment yields (Goode *et al.*, 2012). In addition, there are important differences in timing; management-related sediment is introduced more frequently than fire-related inputs (Istanbulluoglu *et al.*, 2004; Goode *et al.*, 2012), and is most exemplified by chronic loading of fine sediments from forest roads. This distinction has been termed pulsed versus chronic (or press) sediment input (Everest *et al.*, 1987; Yount and Niemi, 1990; Reeves *et al.*, 1995). It has been suggested that chronic disturbances are more detrimental to salmonids than pulsed events because salmonids are better adapted to them (Reeves *et al.*, 1995; Rieman *et al.*, 1997). Consequently, chronic input of fine sediment from roads may pose a greater risk to salmonids than infrequent debris-flow pulses (Goode *et al.*, 2012).

Accepting roads as a greater biological threat can be challenging because the total amount of sediment contributed from forest roads can be several orders of magnitude less than that associated with fire (Goode *et al.*, 2012). Even in heavily roaded basins, yields from roads may only be ~50% of the undisturbed sediment yield and because road sediment tends to be sand or silt size the additional contribution is orders of magnitude below the typical channel transport capacity. While severe impacts to fisheries have been documented after wildfires, there is a capacity for resilience in salmonid species derived from migratory life histories that allows populations to recover after such events (Rieman *et al.*, 2003). The general hypothesis is that wildfire impacts to aquatic habitat are brief and quickly clear away, allowing fish populations to reestablish after disturbance. This hypothesis is supported by results of Megahan *et al.* (1980), who documented rapid habitat recovery following severe fine sediment loading from a major storm in central Idaho.

Is there a disproportionate impact from small, frequently-introduced, sediment loads? This question has some merit in the context of a concentration–discharge relation for sand as discussed by Langbein and Leopold (1968). The implication of their work is that transport rate is in part a function of sediment availability, and the two cannot be considered completely independently (see also Rubin and Topping, 2001). Langbein and Leopold (1968) found concave downward relations between the amount of sand on the bed and the observed transport, demonstrating both the necessity for some sand on the bed for transport to occur and that, after a certain point, no additional sand will increase the volumetric transport rate. Sand travelling over coarser, gravel-bed surfaces may show an even greater dependence of transport on the amount of sand per square meter for low transport rates, and a substantial amount of sand may need to be present even for minimal transport; in the limit, as the amount of sand on the bed becomes small, its mobility may depend on entraining the coarse surface material (Wilcock and Kenworthy, 2002). Although the above studies offer a basic conceptual basis for controls on sand transport, the spatial patterns of sand movement through streams may be an important consideration for aquatic habitat quality and river morphology as well (Grams *et al.*, 2010).

This paper contrasts the physical and biological impacts of sand transport resulting from a single large pulsed event versus a chronic sediment input of equal volume spread over 4 years. The modeling study was done using two-dimensional transport over a gravel bed and considered the consequences for fish reproduction in terms of deposition of fine material on the gravel substrate. A 4-year modeling period was chosen, in part, to represent the salmonid life cycle; disturbances which create unsuitable habitat longer than the salmonid life cycle could affect population persistence. Although chronic loads tend to be smaller than pulsed inputs, we applied the same total loading over 4 years to explore the degree and spatial distribution of impacts to the timing of sediment supply alone. We acknowledge that there may be non-linear interactions between timing and amount, but do not explore those complexities here.

Study Site

The study site is a 1 km long reach of Bear Valley Creek, a tributary of the upper Middle Fork Salmon River in central Idaho, USA (44º N and 115º W) (Figure 1(a)). This site was selected because it represents a typical reach of Bear Valley Creek, with meandering and straight sections, and because it has the potential for receiving chronic inputs from forest roads, as well as pulsed inputs from steeper tributary basins. The stream is typical of low-gradient (<0.5%) gravel-bed channels in the Idaho Batholith that are vulnerable to large inputs of fine-grained sediment as a result of erosion from anthropogenic sources or following natural wildfires. Bear Valley Creek also is ecologically significant as it hosts autumn-spawning Chinook salmon (*Oncorhynchus tschawytscha*) and spring-spawning steelhead (*O. mykiss*) populations; both species are federally listed as threatened. The mean elevation of the stream is about 1950 m and the annual hydrograph is dominated by peak runoff during the early spring–summer snowmelt period with low flow

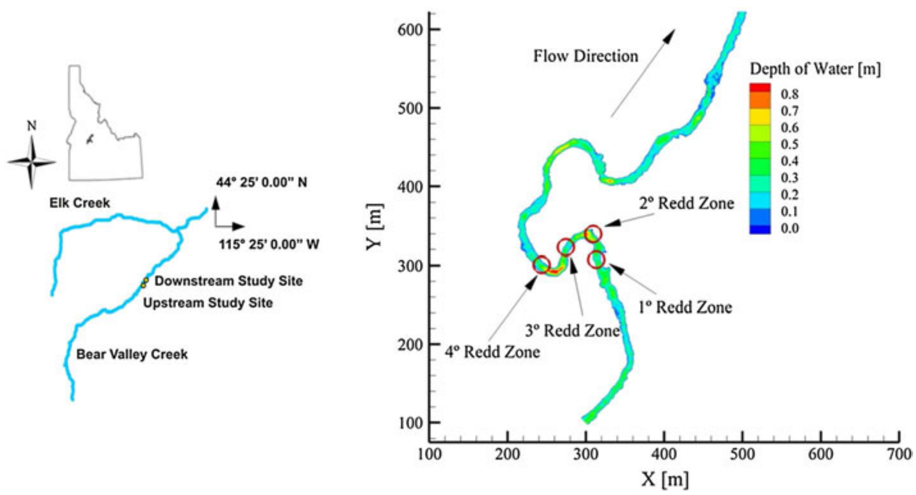

Figure 1. (a) Study site location in central Idaho, USA (modified from McKean *et al.* (2009a)), and (b) study reach, showing redd zone locations and modeled water depths for a low-flow discharge of 1 $m^3 s^{-1}$. This figure is available in colour online at wileyonlinelibrary.com/journal/espl

conditions persisting from August to April. The study reach has a mean bed slope of 0.2% and a mean bankfull width of 15 m, with a straight plane-bed morphology in the upstream section and a meandering pool–riffle morphology along the downstream portion (Figure 1(b)). The channel is unconfined, with a well-developed floodplain, and flows through a wide valley filled with glacial outwash debris. Pebble counts of the streambed surface (Wolman, 1954) indicate a median grain diameter (d_{50}) of 50 mm. Field surveys for the last 15 years (Isaak and Thurow, 2006) identified four recurrent fish spawning sites within the study reach (Figure 1(b)).

Methods

Topography

Detailed topography of the channel and floodplain was obtained using an airborne, bathymetric lidar (McKean *et al.*, 2009a, 2009b). The lidar survey was conducted in October 2007 during low flow with low turbidity, ensuring optimal conditions for the sensor. The lidar data were acquired with a local average density of about 0.5 points/m^2, and were gridded at a 1 m resolution for use in the numerical model. This provides a very detailed and high-resolution map of the stream topography, although some topographic features that change rapidly over short distances (e.g. steep channel banks), may be smoothed by the DEM (McKean and Tonina, 2013).

Hydrology

For our analyses, a scaled average annual hydrograph is estimated from a nearby stream gauge with 30 years of record (1930–1960) (Bear Valley Creek near Cape Horn, ID, USGS gauge 13309000). The gauge is located 20.5 km downstream of the study site. The hydrograph was scaled with a coefficient of 5 to fit the expected bankfull and low flow values of the study site of 6.7 and 1 m^3 s^{-1}, respectively, reported by Tonina and McKean (2010) (Figure 2). Transport is simulated for a 4-year period starting at the beginning of a water year, which starts on October 1 and ends on September 30.

Hydrodynamic model

A two-dimensional numerical model was used to predict coupled changes in flow, bed load transport, channel morphology, and aquatic habitat (Multi-Dimensional Surface Water Modeling System, MD-SWMS; McDonald *et al.*, 2001, 2005; Nelson *et al.*, 2006). Within the MD-SWMS software, we used the FaSTMECH routine (Flow and Sediment Transport with Mechanical Evolution of the Channel), which employs a finite difference solution of the shallow-water equations over a curvilinear grid. Curvilinear grids minimize mesh size as they follow the sinuosity of the channel. Model inputs include discharge (upstream boundary condition), water stage (downstream boundary condition), bathymetry and topography (flow boundary), a roughness coefficient, and a lateral eddy viscosity. MD-SWMS uses an algebraic model for the turbulence closure based on eddy viscosity (Nelson *et al.*, 2006). Although this turbulence closure model is simple and applicable only to boundary-induced homogenous turbulence with low strain, it predicts realistic velocity distributions because turbulence is primarily induced by flow-boundary interactions in natural streams (Nelson *et al.*, 2003). Additionally, this closure approach produces rapid numerical convergence and is stable, allowing a reasonable computational time for morphodynamic analyses. A sub-model accounts for secondary flows, which have important effects on the direction and magnitude of the boundary shear stress (Nelson and McDonald, 1997; Nelson *et al.*, 2003; May *et al.*, 2009). Thus, MD-SWMS is effectively a pseudo three-dimensional or 2.5-dimensional model (Tonina and Jorde, 2013).

Figure 3 shows the initial reach topography determined from the lidar survey interpolated to a curvilinear grid. For an observed discharge of 0.98 m^3 s^{-1}, we calibrated the boundary roughness length scale z_0 as $0.12d_{50} = 0.006$ m, which is the height above the bed where the velocity profile goes to zero (Tonina and McKean, 2010; McKean and Tonina, 2013). The z_0 value was assumed constant; z_0 scales with the coarse fraction of the bed material (Whiting and Dietrich, 1990; Wiberg and Smith, 1991) and does not change with discharge unless there is a corresponding change in the size of the coarse mate-

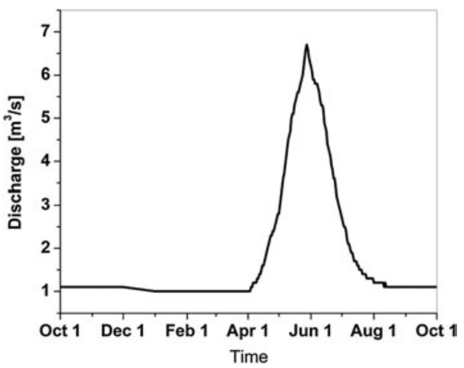

Figure 2. Annual hydrograph used for hydraulic and sediment transport computations within the study reach.

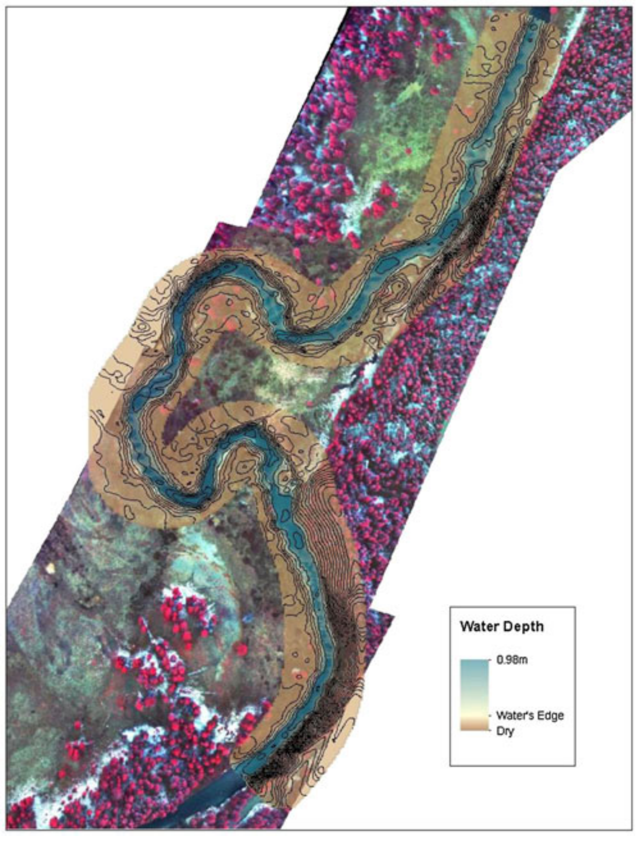

Figure 3. Channel topography based on a curvilinear grid, overlain on aerial photographs of the site. Solid lines are contour intervals of 0.3 m, blue and brown shades indicate water depth and exposed topography, respectively, for the 0.93 m^3 s^{-1} discharge. This figure is available in colour online at wileyonlinelibrary.com/journal/espl

rial on the streambed. Nevertheless, a constant z_0 still allows flow resistance to change locally with discharge, because the resistance coefficient (C_d) is a function of flow depth (McDonald *et al.*, 2005). We assumed that the lateral eddy viscosity, ν, was spatially constant within the reach and estimated it as $\nu = 0.01 \cdot U \cdot H$, where U and H are the mean flow velocity and depth at the reach scale (Barton *et al.*, 2005). Good agreement was observed between measured and predicted water surface elevations (Figure 4(a)) and between measured and predicted mean velocities (Figure 4(b)) for the calibration discharge (0.98 m^3 s^{-1}). Because changing the value of the lateral eddy viscosity within the range of flows investigated in this work produced negligible changes in transverse flow structure and water surface elevation, we adopted a constant value for of 0.05 m^2 s^{-1}, which also ensures model stability at both low and high flows. After selection of constant values for ν and z_0, we predicted the velocity distribution over a range of discharges between 1 and 6 m^3 s^{-1} for which we had field measurements at two cross-sections. Comparison between simulated and measured values of mean velocity showed good agreement, with errors comparable with those found in literature (Figure 4(c)) (Tonina and Jorde, 2013).

The flow mesh of the study reach is composed of 90 × 800 cells, with cell width and length equal to 0.5 and 1 m, respectively. A sensitivity analysis shows that this grid configuration well predicts flow structure and improves solution convergence. For example, the model captures the size and location of two observed eddies generated at two bends. Solution of the hydraulic model is accepted if the convergence is between ±3% of the water mass in each cross-section. Flow structure and velocity intensity did not change with smaller grids and consequently the results are mesh-independent.

Sediment transport model

We modified the FaSTMECH routine to use Wilcock and Kenworthy's (2002) two-class bed load transport equation to examine the transport of sand over the armored streambed of the study site (Appendix 1). This two-class equation predicts sand transport with accuracy comparable to multi-class equations, but has the advantage of requiring less grain-size information (Tonina *et al.*, 2007). We set the representative diameters of the coarse and sand classes equal to 50 mm (d_{50} of the site) and 2 mm, respectively, with the sand class representative of both the pulse and chronic supplies. We assumed that sand is mobile over an immobile gravel bed because field observations and previous numerical simulations show that the armor layer is largely stationary in Bear Valley Creek even at bankfull discharge (Tonina and McKean, 2010; McKean and Tonina, 2013).

Field measurements showed very low sediment transport in Bear Valley Creek at near-bankfull flow and safety concerns prevented measurements during bankfull conditions. Therefore, the Wilcock and Kenworthy (2002) equation was tested against sand transport observed in Valley Creek, a nearby stream with characteristics similar to Bear Valley Creek. King *et al.* (2004) measured bed load transport in Valley Creek over a 3-year period in a fairly straight reach. Transport was measured over a range of discharges from low flow to over bankfull at 10 equally spaced stations along a single transect using a Helley–Smith bed load sampler with standard 3 inch (76.2 mm) and 6 inch (152 mm) square nozzle entrances for low and high flows, respectively. The location of the transect varied between events. Bed load was sampled in two passes along the transect, for a total of 20 point measurements lasting 30–60 s each, with all data subsequently combined for a given flow event. We compared the observed transport rates with those predicted from the Wilcock and Kenworthy (2002) equation using reach averaged depth and width for each discharge measurement to define the shear stress because detailed topographical information required to run the 2D FaSTMECH model was not available. To account for only the grain roughness portion of the bottom shear stress we used the Einstein–Keulegan resistance equation (Appendix 2) with the streambed roughness estimated as $2d_{90}$ (Whiting and Dietrich, 1990). Comparison between observed and predicted sand transport shows reasonable agreement across a range of discharges

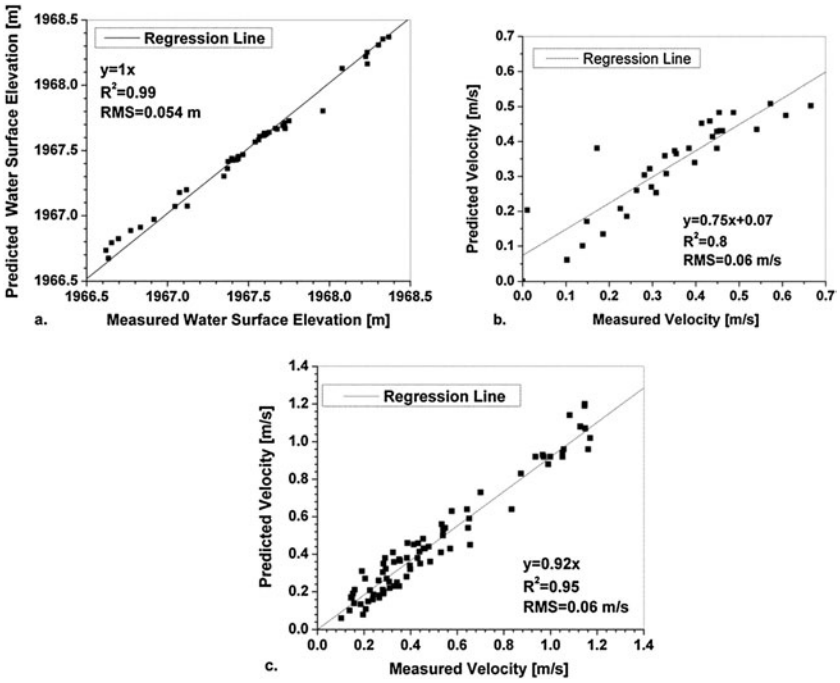

Figure 4. Comparison between model predicted and observed (a) water surface elevation and (b) depth-averaged mean velocity at the calibration discharge of 0.93 m^3 s^{-1}. The panel (c) shows the validation of the model with depth-averaged mean velocity for a range of discharges between 1 and 6 m^3 s^{-1} (from McKean and Tonina, 2013).

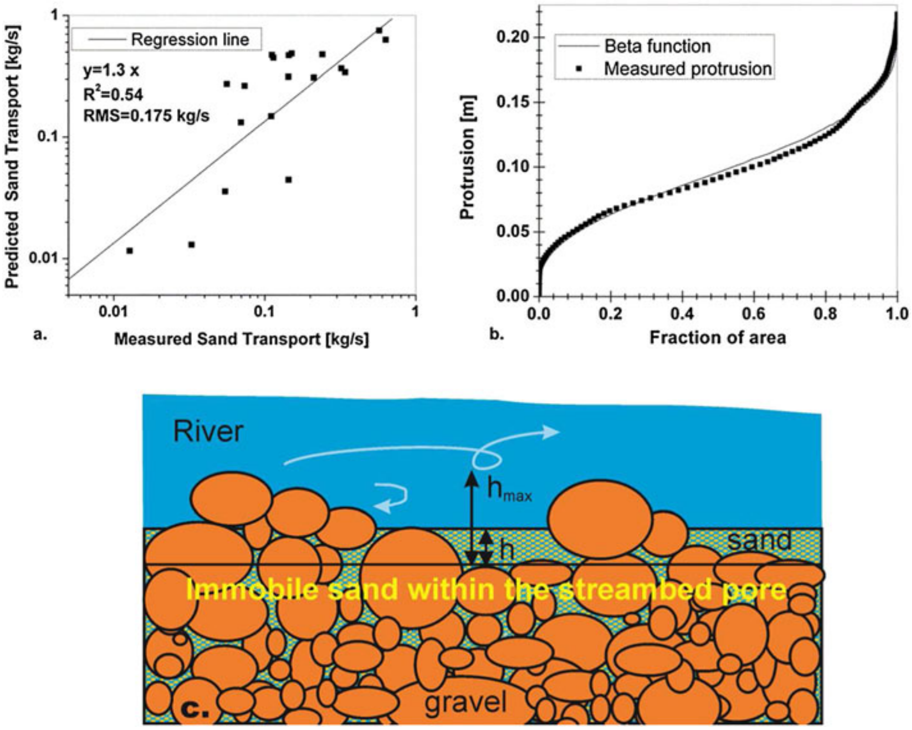

Figure 5. (a) Comparison between measured and predicted sand transport in Valley Creek, Idaho using the Wilcock and Kenworthy (2002) equation (Appendix 1). Valley Creek has a channel morphology similar to Bear Valley Creek (King *et al.*, 2004). (b) Comparison between measured and estimated protrusion for the Payette River near Horseshoe Bend, Idaho using a beta function (Equation 1). (c) Sketch of sand deposition over the coarse material. The horizontal black line indicates the depth of the surface layer ($h_{max} = 2d_{50}$), below which sand is immobile and above which is mobile. This figure is available in colour online at wileyonlinelibrary.com/journal/espl

between 4 and 10 m^3 s^{-1} (Figure 5(a)). While this provides support for our use of the Wilcock and Kenworthy (2002) equation, no data were available to test the subsequent FaSTMECH predictions of 2D bed load transport.

Mode of transport

The dimensionless Rouse number, $R_s = \frac{\omega_s}{\kappa u_*}$, was used to estimate the mode of particle transport, where ω_s is the settling velocity calculated using Dietrich's (1982) approach, κ is von Kármán's constant (0.408; Long *et al.*, 1993), and u_* is the shear velocity $u_* = \sqrt{\tau_b/\rho_w}$, where τ_b is the boundary shear stress (predicted by the model) and ρ_w is the water density. According to the Rouse number, a grain is expected to move as bed load when $R_s > 2.5$, partly as bed load when $1.2 < R_s < 2.5$, totally in suspension when $0.8 < R_s < 1.2$, and as wash load when $R_s < 0.8$ (Bagnold, 1966; Cheng and Chiew, 1999). A set of preliminary simulations, using the full hydrograph (Figure 2), was used to estimate R_s values for sand in each grid cell. Results show $R_s > 2.5$ for the entire domain at all flows, implying that sand moves primarily as bed load in this reach.

Sand deposition

Because coarse material is assumed immobile fine sediment can deposit over the irregular surface defined by the coarse sediment, but cannot be moved from the subsurface layer (Figure 5(c)). To account for deposition of sand on the streambed, we model grain protrusion and the corresponding voids available for storing sand. The model assumes that sand deposits within the voids of the streambed surface without changing the streambed topography until the voids within a surface layer 2 x d_{50} in thickness are completely filled. We also assume the streambed voids are initially empty within this armor layer. Once sand entirely covers the coarse material within a numerical cell, the streambed morphology may change and new streambed elevations are updated within the numerical domain. We further assume that the subsurface voids below the $2d_{50}$ armor layer are completely filled with sand.

Particle protrusion is predicted from a beta distribution that depends on the mean, μ, variance, σ, and maximum height, h_{max}, of the streambed sediment protrusion (Tonina *et al.*, 2007). The beta function with the protrusion, h, normalized by h_{max}, $h' = h \cdot h_{max}^{-1}$, has the following form:

$$f(h') = \frac{\Gamma(p+q)}{\Gamma(p)\Gamma(q)} h^{p-1}(1-h')^{q-1} \quad (1)$$

where $\Gamma(x) = \int_0^\infty \tau^{x-1} e^{-\tau} d\tau$ is the Euler gamma function and depends on μ and σ, the two shape parameters of the beta function. The variable x stands for p, q, or $p+q$ and τ is the integral dummy variable; $p = \mu\gamma$ and $q = (1-\mu)\gamma$, where $\gamma = \frac{\mu(1-\mu)}{\sigma} - 1$. Figure 5(b) compares measured and estimated protrusion values for the Payette River near Horseshoe Bend, Idaho, and verifies our mathematical approximation of the protrusion. In our study reach, the three parameters, μ, σ and h_{max}, are estimated from pebble counts of the surface material, yielding values of 6, 3.4 and 12 cm, respectively.

Because observed protrusion distributions are not available for the study site, we conducted a sensitivity analysis for the predicted protrusion values. Results of numerical simulations in which we allowed μ, σ and h_{max} to vary by ±30% show differences in sand spatial distribution of less than 17%, and average sand volume changes within a numerical cell of less than 10%, suggesting a robust model. Differences in sand spatial distribution are quantified by the percentage of cells that change between having and not having sand because of varying the above parameters. Most of the cells that changed their sand content status were at the fringe of sand bars and sand transport paths and had, at the most, very small volumes of sand, resulting in negligible effects on the overall sand distribution.

These errors are similar to those quantified by varying the size of the sand diameter by 50%. A sediment pulse with a 50% larger representative sand diameter (2.5 mm) presented differences in sand spatial distribution of less than 6%, and average sand volume changes within a numerical cell of less than 4%. The coarser sand pulse showed less transversal dispersion than that of 2 mm sand. Conversely, a sand pulse of 50% finer sand (1.5 mm) had a larger error than that of the coarser pulse. Differences in sand spatial distribution were less than 20%, with average sand volume changes within a numerical cell of less than 6%. Again, most of the changes were at the fringe of the pulse where there were very small amounts of sand.

Sediment supply

Our goal is to study the effects of chronic and pulse sediment supplies under the condition of maximum sediment delivery to the study reach, which is dependent on the transport capacity of the reach and, in particular, the upstream cross-sections. Simulations show that defining an upstream input greater than capacity causes sand to deposit in the first cells of the numerical domain, causing aggradation that decreases transport to the rest of the reach compared to an at-capacity input. Application of the Wilcock and Kenworthy equation (2002) at the study site indicates an annual reach transport capacity for sand of about 20 m^3 yr^{-1}. Based on this analysis, we set the annual chronic supply of sand equal to 20 m^3 yr^{-1}, and the pulse supply equal to 80 m^3 giving equal total inputs for both scenarios over the 4-year modeling period. We also ran two additional scenarios of 40 and 140 m^3 to investigate the impact of pulse size on pulse evolution. A set of pilot simulations that indicate evacuation of the pulse sediment would take decades at sites such as ours. The sand moves quite slowly in these systems and mostly forms lateral sand bars

In comparison with typical debris-flow events in the study area, a sediment pulse of 80 m^3 would be a fairly small event; comparable with a small tributary debris flow or a small hillslope failure. For example, post-fire debris flows in the study area from basins on the order of 10 km^2 have produced deposits containing several hundred to several thousand cubic meters of sediment (Cannon *et al*., 2010; Goode *et al*., 2012). However, field observations indicate that much of this material never moves after deposition and is stored in debris fans or as alluvial fill within the river valley. We do not suggest that a sediment pulse of 80 m^3 is a typical event size for our study area, but rather explore how a single input event would contrast to one where inputs were distributed over time. Given that the channel transport capacity limits what can be mobilized, a larger event would result in a large amount of sediment being left at the point of entry. Our modeling explores only what happens downstream of such an event, which necessarily depends on how much material can be eroded from the event deposit.

Preliminary simulations also show that the location where sediment transport is started had an effect if it was at riffles or in pools, whereas location is less important in a straight gently-varying reach. The former areas tended to limit the sediment transport and so less sand moves into and through the model domain. Beginning the transport simulations in a straight smooth reach promotes an almost uniform sediment flux, both transversally and longitudinally, and allows more sand to enter the system. The upstream portion of our study reach provided this sort of ideal condition for input and is below a tributary confluence that is a potential source of fine sediment.

The sand pulse was placed over a streambed area that is 30 m long by 7 m wide to allow full accommodation and submergence of the pulse within the channel (Figure 6(a)). This initial spatial distribution of the pulse is necessary because modeled transport can occur only in submerged cells and its location 200 m below the upstream end of the study reach was chosen to facilitate numerical stability of the model. In contrast, the chronic supply entered the reach across a 7 m wide cross-section located 10 m below the upstream end of the model domain (Figure 6(b)). This cross-section was selected for the chronic input location to prevent instabilities in the hydraulic model due to rapid changes of streambed geometry over the first 10 m of the study reach, as discussed above. The annual 20 m^3 chronic supply was introduced as a constant percentage (10%) of the instantaneous transport capacity of the input cross-section, and thus the daily input changed as a function of discharge throughout the year. As such, the chronic supply is treated as a transport-limited input of material to the study site from the upstream river and it increases with discharge. We assumed that initially there was no sand within the reach.

Analysis of model results

The predicted spatial distribution of sand, its depth, changes in streambed elevation and influence on the substrate composition (i.e. percentage of sand) were used to evaluate channel and habitat response under both sediment input scenarios. In the spawning zones (Figure 1), the fraction of sand within a redd was calculated by dividing the predicted mass of sand by the mass of coarse material over a depth equal to $2d_{50}$ of the coarse material; calculations were performed over typical

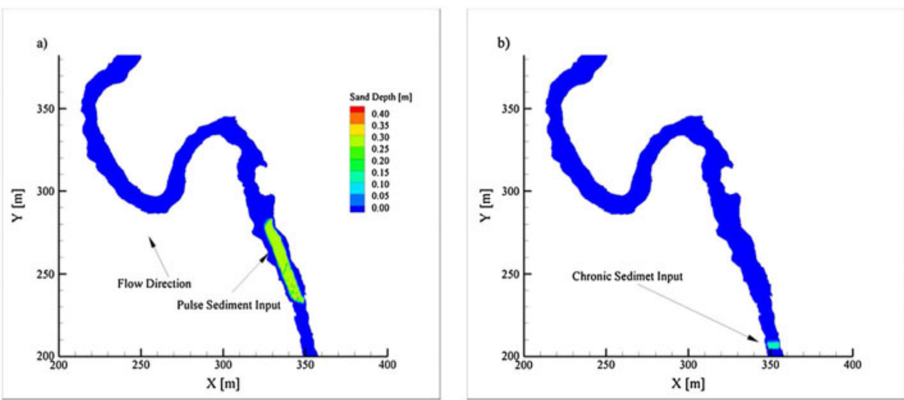

Figure 6. Initial conditions for (a) pulse and (b) chronic sediment inputs. This figure is available in colour online at wileyonlinelibrary.com/journal/espl

areal dimensions for redds (10 m^2 for Chinook salmon, 5.4 m^2 for steelhead; Bjornn and Reiser, 1991).

The predicted movement of the sand pulse was also examined to investigate whether the pulse moved by advection, diffusion, or a combination of these two processes; an issue that has been debated in previous studies of sediment pulses (Lisle *et al.*, 1997, 2001; Cao and Carling, 2003; Cui *et al.*, 2003a, 2003b; Cui and Parker, 2005). To examine this, we monitored the pulse center of mass and the variance of the spatial distribution of sand within the study reach. The center of mass and variance of the sand pulse were calculated based on sand volume present at each cell at a given time in the curvilinear coordinate system. Although we could define these statistics along both the longitudinal and transverse directions, we analyzed and reported only the statistics along the longitudinal direction because that shows the movement of the pulse along the stream network.

Results

Sediment transport and morphodynamics

Pulse input

Figure 7 shows the spatial distribution and depth of sand after each modeling year (weeks 52, 104, 156 and 208), as well as locations of three bars formed by the sediment pulse. Bar 1 develops from the lag material of the sand pulse. Bar 2 forms after 32 weeks, followed by Bar 3 approximately 5 weeks later (week 37). Bar 1 maintains its shape and position during the entire simulation period, with its thickness decreasing only during peak flows when it is entirely submerged. Bar 1 remains partially dry at low flows and thus during those periods it does not change. Bar 2 forms upstream of an ephemeral island, while Bar 3 grows in the inner part of the first bend and opposite a pool. Bars 2 and 3 remain at the same positions during the entire simulation period, preserving their shape and having average sand depths of 0.1 and 0.15 m, respectively. Simulations for the 40 and 140 m^3 sand pulses predict similar morphological evolutions and sand depositional areas, but with lower and higher local sand thicknesses, respectively, than that of the 80 m^3 case.

Figure 7 also shows the sand path along the model domain. The sand introduced from the pulse rapidly spreads throughout the reach, with the locations of thick sand deposits shifting from one bank to the other in the meandering portion, following the direction of high shear stresses. This pattern shows that sand travels around pools in the meandering section, building Bar 3, which prevents sand from entering the adjacent pool as bed load.

Figure 8 shows the position of the center of mass of the pulse and the variance of the spatial distribution of sand within the study reach over the first 2 years of the simulation using three different pulse volumes. The upper curve in each plot represents the hydrograph and the lower curves show the positions of the center of mass (Figure 8(a)) and the variance of the distribution of sand (Figure 8(b)). The initial position of the center of mass is approximately 200 m downstream of the upstream end of the study site (Figure 6(a)). After entering the stream, the center of mass immediately moves downstream 4.2 m during base flow (weeks 1 and 2), without any changes in the spatial variance of sand. Thus, the pulse initially exhibits translational motion (i.e. advection). After these initial changes, and still at base flow, the center of mass moves 3 m downstream and the

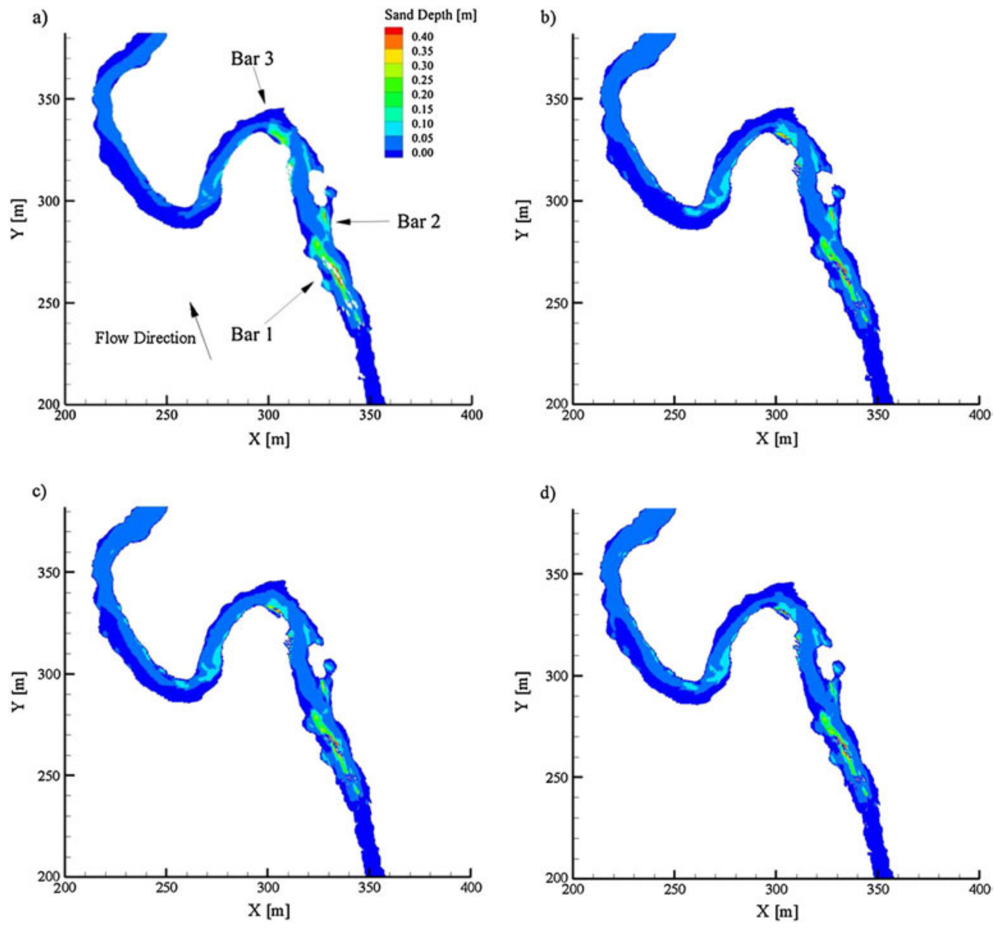

Figure 7. Location and depth of sand at the end of each model year (a–d) following a single pulse input of 80 m^3 of sand. Sand bars formed by the pulse are also shown. This figure is available in colour online at wileyonlinelibrary.com/journal/espl

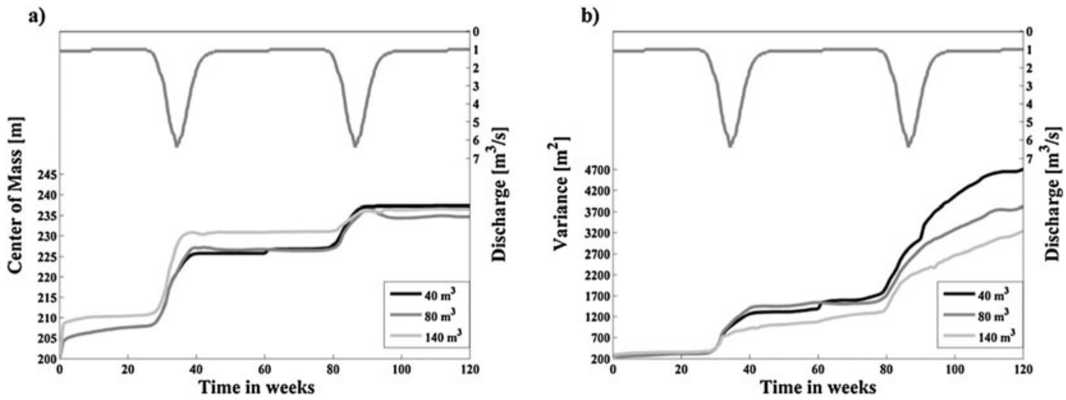

Figure 8. Evolution of (a) the center of mass and (b) the variance of the spatial distribution of sand within the study reach for a sediment pulse of 40, 80 and 140 m^3. Discharge is plotted at the top of each panel over a 2-year period.

variance increases slightly (200 m^2) (weeks 2–26), suggesting that both advection and dispersion processes are taking place, albeit slowly. However, as the discharge rises with spring snowmelt, the center of mass moves downstream quickly and the variance rapidly increases (weeks 26 to 45). The pattern of displacement is similar in all three pulse volumes, however the largest pulse shows a consistently larger displacement. During the recession portion of the hydrograph, both the center of mass and variance level off, indicating a decrease in both advection and dispersion processes. Overall, the center of mass moves 20 m during the first high flow. As discharge returns to base flow, the center of mass remains stationary, with the variance increasing slowly, suggesting a purely dispersional process during the falling limb of the snowmelt peak.

The behavior of the center of mass during the second year of high flows is similar, but shows less displacement than that of the first year. This is because sand is accumulating in point bars, especially around the first bend, which slows downstream migration of the pulse. After the peak discharge of the second year, the pulse center of mass is roughly stationary, while the variance of the distribution of sand substantially increases, suggesting that motion of the sand is primarily diffusional during this time. The amount of diffusion also varies inversely with the size of the pulse. This behavior could be due to the non-linear effect of the hiding function in the Wilcock and Kenworthy (2002) bed load transport equation. A lower fraction of sand causes a higher Shields number because the sand is better sheltered by the coarse material. Thus, small fractions of sand move slower than large fractions. The variance of the distribution of sand behaves differently during the receding limbs of the first and second year hydrographs. This is probably due to bar formation and associated sand storage in the first year (Figure 7(a)), followed by winnowing of the point bars and the subsequent release of sand in the second year, causing an increase in the spatial variance of sand. The variance levels off for the two smaller pulses when the sand reaches the end of the modeling domain and starts leaving the study site (week 122). The apparent slight upstream movement of the center of mass on the falling limb of the second peak discharge (weeks 90–95) is within the 1 m resolution of the numerical mesh and is likely a rounding error. The variance and center of mass of the plume cannot be estimated after year 2 because some sand leaves the study site.

Chronic input

Figure 9 shows the spatial distribution and depth of sand along the study reach after each modeling year (weeks 52, 104, 156 and 208) for the chronic supply. Results indicate the formation of four bars, labeled Bars 1, 2, 3 and 4 in Figure 9, that form at the 10th, 14th, 35th and 39th week, respectively. The first two bars develop on the left bank of the straight portion of the stream. They correspond to areas of re-circulating flow (eddies), where flow diverges due to small bank cavities. These two depositional sites were in the source zone for the pulse input (see Figure 6(a)) and thus no bars formed there during the pulse input simulation. All bars maintain their locations until week 104, but they change in shape and size. For example, sand thickness of Bar 1 increases approximately 0.1 m between weeks 52 and 104. After the 104th week, Bars 1 and 2 are removed from the stream, but Bar 1 forms again at week 156.

Similar to the pulse input, sand spreads over the entire stream width along the straight reach, and shifts from bank to bank in the meandering section, as it follows the inner part of the bends and bypasses the pools.

Spawning site analysis

Figures 10 and 11 show the percentage of sand in the upper 10 cm of the substrate for the pulse and chronic supplies within the four spawning areas of the study reach shown in Figure 1(b). The limits for egg to parr survival as a function of fine sediment amount are also shown for Chinook and steelhead (Rhodes *et al*., 1994).

For a pulse input of sand, survival decreases to less than 3% during the first year for Chinook embryos at spawning site 1 due to the proximity of this site to the sediment input, but otherwise the percentage of sand does not reduce the egg to parr survival below 29% for either species (Figure 10). On the other hand, results of the chronic scenario indicate decreased survival for Chinook embryos at spawning site 1 during the first and third years (3% and 13% survival, respectively); whereas, survival of steelhead embryos is always greater than 29% (Figure 11). For both species, the chronic supply increases mortality compared with the pulsed supply at spawning site 1 in nearly all years. Mortality at spawning sites 2–4 is negligible for both sediment supply scenarios.

In both scenarios, the percentage of sand shows periodic changes that mirror the hydrograph, indicating that the sand is mobile (rather than trapped in gravel interstices) and responsive to flow. Thick deposits of sand form at the spawning sites during high flows, but sand is removed from the surface of the bed during the receding limb of the hydrographs similar to the results of Wu (2000) and Wu and Chou (2003). Sediment transport increases in the entire domain with discharge and fine sediment converges toward the riffles following the path of higher shear stress. However, as discharge decreases, sand is stored in the bars, which become dry, and shear stress decreases faster in the rest of the domain than in the riffles, such that less fine sediment enters the riffles, where high shear

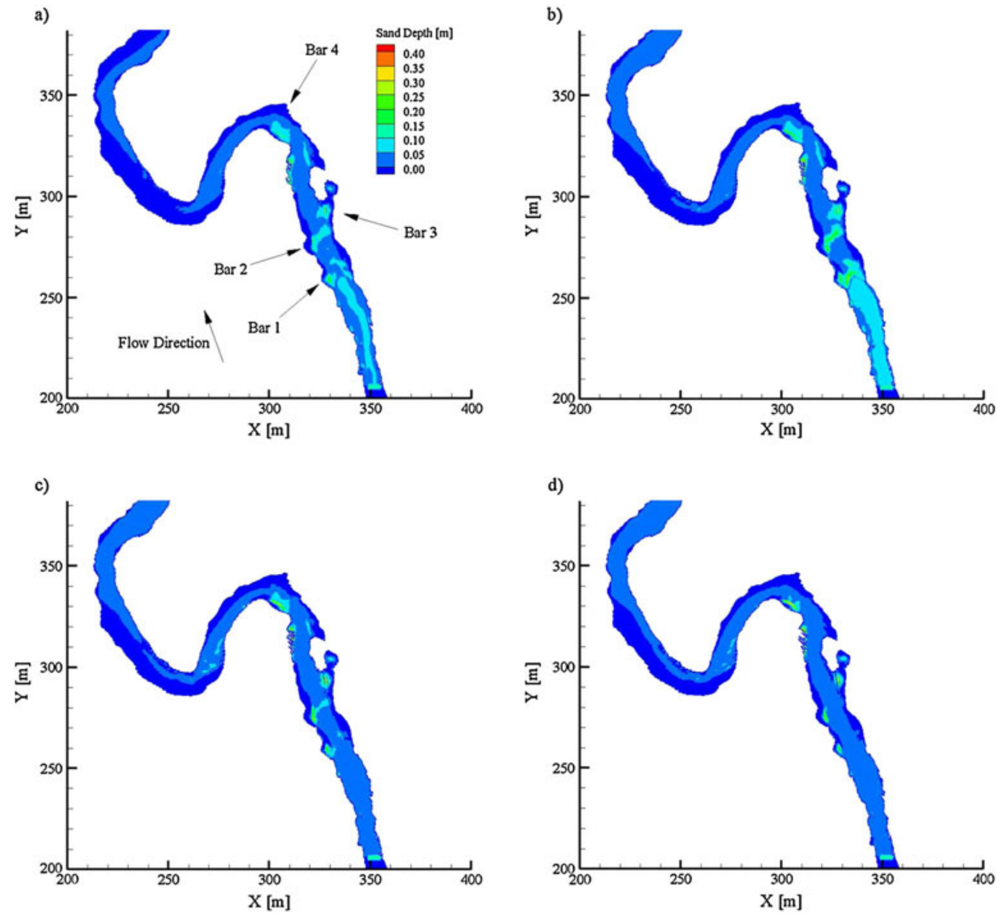

Figure 9. Location and depth of sand at the end of each model year (a–d) due to a chronic input of sand. Sand bars formed by the chronic supply are also shown. This figure is available in colour online at wileyonlinelibrary.com/journal/espl

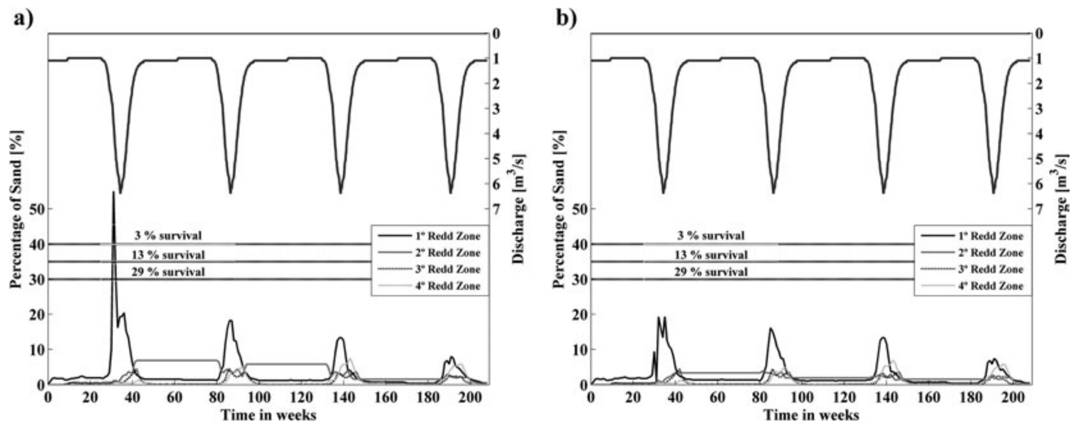

Figure 10. Percentage of sand deposited in the spawning zones (Figure 1) during the pulse supply, showing 3, 13 and 29% limits for egg to parr survival (Rhodes *et al.*, 1994) for (a) Chinook and (b) steelhead salmon. Annual hydrographs are also shown at the top of each panel.

stresses are able to transport most of the fine sediment. This sediment transport gradient on the falling limb of the hydrograph allows for the decrease of fine sediment within spawning sites due to their location near riffles.

Discussion

Channel response is similar for both sediment supply scenarios. The sand spreads downstream, is responsive to changes in flow, and builds sand bars. In both supply scenarios, two of the sand bars have similar shapes, thicknesses, and locations; one at the beginning of an ephemeral island (Bar 2, Figure 7; Bar 3, Figure 9) and the other forming a point bar in the first meander (Bar 3, Figure 7; Bar 4, Figure 9). These modeled features correspond well in size, shape and location with deposits seen in the field at this study reach. The first bar develops upstream of the ephemeral island because sand is trapped and deposited by local hydraulics. The island is an obstacle to the flow, causing flow deceleration and sand deposition in a stagnation zone at the upstream end of the island. In contrast, the second bar results from secondary flows in the meander bend (Dietrich and Smith, 1983, 1984). Shear stress vectors point inward at the bend concentrating fine sediment in the inner part of the meander, where sand accumulates, forming the point bar. The fact that similar bars form in both supply scenarios suggests that

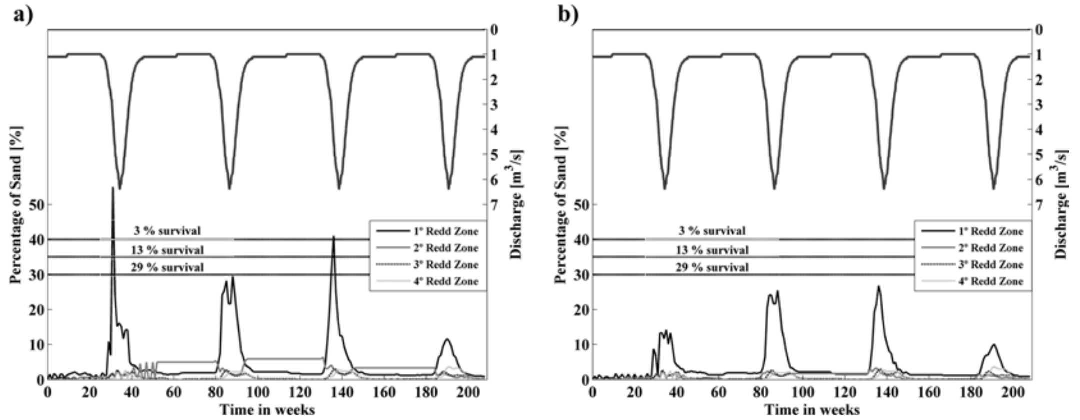

Figure 11. Percentage of sand deposited in the spawning zones during the chronic supply, showing 3, 13 and 29% limits for egg to parr survival (Rhodes *et al.*, 1994) for (a) Chinook and (b) steelhead salmon. Annual hydrographs are also shown at the top of each panel.

these features are forced by site-specific characteristics of the channel (i.e. the presence of an island and meander bend). Furthermore, results show that the sand mass stored at these bars is similar for both supply scenarios. In contrast, sand bars that are not common to each supply scenario likely reflect the scenario itself (e.g. the large lag bar at the site of the sediment pulse and Bars 1 and 2 in the chronic scenario that are within the pulse supply area).

Sand deposition does not strongly impair the spawning zones in either supply scenario, except for the first spawning site, which is the closest to the sand source (Figures 10 and 11). Consequently, the quality of the spawning habitat is highly dependent on the location of the sediment input, with sites close to the sediment source having a higher risk than those farther downstream. The three downstream spawning areas are located in the meandering section of the channel (Figure 1), where sand deposition occurs mainly along the periphery of pools during low flows (Figures 7 and 9). This topographic steering of the sediment flux minimizes sand deposition upstream of riffles, suggesting that this topography may shield spawning sites from large amounts of sand transport and deposition, effectively reducing the probability of redd entombment. Consequently, the underlying reach morphology may be an important modulating factor for the effects of sand loading to streams. Although both pool–riffle and plane-bed morphologies offer suitable gravel and cobble substrate for salmonid spawning, the hydraulics of meandering pool–riffle channels may minimize impacts to spawning zones, compared with hydraulically homogeneous plane-bed channels.

In the first spawning zone, the chronic supply causes greater embryo mortality than the pulse supply across all years and is more persistent (Figures 10 and 11), supporting our hypothesis about the relative impacts of each sediment input scenario. However, the ecological impacts differ for the two salmonid species examined here. For Chinook salmon, the greatest mortality occurs in the first year in both supply scenarios, while the impacts to steelhead embryos are less variable between years. The smaller surface area of the steelhead redds has lower fine sediment deposition than in Chinook redds. This is because fine sediment is not deposited uniformly at riffle spawning sites and the large Chinook redds capture areas with thicker deposits than the smaller steelhead redds.

We did not consider an important aspect of biophysical interactions that occur each year at spawning sites. During construction of spawning nests, female fish lift the surface and shallow subsurface materials into the flow, which loosens the large particles and winnows away fine sediment. This annual process may reduce the impact of both chronic and pulse fine sediment supply in spawning areas, especially if flows are low with minimal sand transport after spawning as is the case for Chinook salmon in Bear Valley Creek.

In both sediment supply scenarios, transport-limited input of sand causes the percentage of fine material to vary directly with the hydrograph, and is greatest during peak flows. This has implications for altered hydrology due to climate change. Climate studies predict that warming in the western USA will cause smaller snow packs, and potentially larger flood flows from increased rain or rain-on-snow events during the winter season in high mountain watersheds like the study site (Barnett *et al.*, 2004, Mote *et al.*, 2005, Goode *et al.*, 2013). Consequently, under conditions of high sediment loading, climate-related increases in flow during periods of egg incubation could enhance overall sand mobility and cause greater embryo mortality from sand deposition.

Analysis of the movement of the sand pulse indicates that the center of mass of the pulse moves only 40 m in 120 weeks (Figure 8(a)). This suggests that recovery from sand pulses may require decades in low-gradient, meandering channels, such as that examined in this study. Initially the flow works rapidly on the sand pulse, creating bars and distributing the sediment along the stream, with the largest changes occurring during the spring flood, and with motion of the pulse exhibiting a mixture of both advection and dispersion (Figure 8). Once the major bars are formed, advection of the center of mass slows down and dispersion is the prevailing transport mechanism. This finding supports the results of Cui and Parker (2005), who showed that dispersion is the main sediment transport process in mountain streams. This conclusion is also supported by field studies, flume experiments, and most one-dimensional numerical simulations (Lisle *et al.*, 1997, 2001; Hansler, 1999; Cui *et al.*, 2003a, b).

Flume experiments by Humphries *et al.* (2012) also showed that the sediment pulse may move by a combination of translation and diffusion with their relative importance depending on hydrograph shape and peak magnitude. Our results and the laboratory experiments of Humphries *et al.* (2012) also show that the sediment transport changes with successive flood events because of the interaction between streambed morphology and sediment pulse evolution. As observed in their flume experiments, pool–riffle morphology affects the sediment pulse movement with sediment depositing in point-bars. As sediment accumulates, it changes the sediment flux at that section, which in turn controls how sediment moves through the stream reach. Conversely, Cui *et al.* (2003a, 2003b) observed that pulses of fine sediment primarily translated rather than diffused under constant flow in a straight reach. Thus, unsteady discharge and complex channel topography with high sinuosity may promote diffusion over translation. We observe that the relative importance of diffusion increases over translation with successive hydrographs. This suggests that not only hydrograph shape, but also the sequence of hydrographs, may be important.

In contrast to the results from the flume experiments of Sklar *et al*. (2009), our model predicts that the relative importance of dispersion over translation decreases with increasing pulse size. This different behavior could be due to the combined effects of an unsteady hydrograph and the complex meandering topography considered in our study. Sklar *et al*. (2009) used a constant discharge through straight featureless topography. Consequently, we suggest that initial stream topography may have a key role in modulating fine pulse evolution at least in low-gradient gravel-bed rivers.

Our analysis considers bed load transport only, which is appropriate in our case based on calculated Rouse numbers and the associated mode of transport. However, suspended transport may be an issue for finer sediment inputs, or for steeper channels, and may yield different patterns of sediment transport, deposition, and ecological impact. We did not calibrate the Wilcock and Kenworthy (2002) bed load transport equation to our particular study site, because no transport measurements were available. Uncalibrated bed load transport equations can introduce substantial errors in flux magnitude (Gomez and Church, 1989; Barry *et al*., 2004). However, the Wilcock and Kenworthy (2002) equation accurately predicted sand transport in a nearby stream with channel characteristics similar to the study reach (Figure 5(a)).

Our results are applicable only to cases where the fine sediment supply is fully submerged on the channel bed. Lateral erosion of dry bars or other sediment sources is not included in the model and erosion or deposition occurs only in wet, entirely submerged cells. We recognize that pulse supplies often originate from debris-flow fans that extend into the main channel and that erode primarily along their distal margins. In contrast, our sediment pulse is distributed across and along the channel bed (Figure 6(a)), thus exposing just the top surface, rather than the distal margin, to erosion. Roughly 25% of the pulse remains in place on the channel bed at the end of our 4-year simulation. In contrast, the equivalent chronic supply is fully exposed to the flow as it is introduced and is thus potentially more mobile. This likely explains why the fine sediment concentration from the chronic supply is more sustained at the first redd site than that of the pulse input (Figures 10 and 11).

Conclusions

The aquatic habitat of streams is often quite sensitive to the amount and composition of fluvial sediment (Cummins and Lauf, 1969; Buffington *et al*., 2004). Some habitat elements, such as egg nesting and incubation sites for salmonids, are particularly vulnerable to fine-grained sediment. In this study, we used a modified multi-dimensional flow model and examined whether the style of fine sediment supply, specifically acute pulses versus steady chronic inputs, influenced the transport and deposition patterns of fine sediment and their effects on egg nests. Results show a broadly similar spatial pattern of sand transport and deposition in response to the two sediment supply scenarios. The major control on transport is the seasonal hydrograph. Results show that in this system large flow events may be detrimental for redd habitat not because of the risk of scour, but due to sand transport and burial of egg nests, similar to the findings of May *et al*. (2009). However, the channel topography strongly influences depositional patterns and reduces the impact of sand on the egg nest sites in channel riffles. The downstream redd closest to the sediment input location was most strongly impacted by sand in both supply scenarios and, as expected, the chronic supply had more severe and persistent effects.

Our results show that dispersion is the major transport mechanisms of sediment pulses of fine sediments. The relative importance of dispersion over advection decreases with increasing pulse size.

The sediment input model could be improved to include lateral erosion around the margins of semi-submerged sediment sources. This would allow sediment to be introduced on the margin of a channel, in the style more typical of debris flow-generated sediment pulses.

Future work examining the role of channel morphology in modulating ecological impacts of fine sediment is also warranted, as well as examining the effects of supply magnitude relative to transport capacity to investigate questions such as how much sand must be introduced before bar deposition is overwhelmed and sand begins to fill the pools. Once filled, what kinds of flows and time are required to remove sand from pools?

Acknowledgements—Funding for this research was provided by the US Forest Service through the National Fire Plan and the Rocky Mountain Research Station, Boise, Idaho. We thank the associate Editor, Jim Pizzuto, and two anonymous reviewers for their comments on an earlier version of the manuscript.

Appendix 1

The Wilcock and Kenworthy (2002) two-class bed load transport equation has the following form:

$$q_{bi} = \frac{\rho_s F_i u_*^3}{\Delta g} q_{bi}^*$$
$$q_{bi}^* = \begin{cases} 0.002\phi_i^{7.5} & \text{for } \phi_i < \phi' \\ A'\left(1 - \dfrac{\chi}{\phi_i^{0.25}}\right)^{4.5} & \text{for } \phi_i \geq \phi' \end{cases} \tag{A1}$$

where q_{bi} is the mass bed load transport rate per unit width for the *i*th size class (sand or gravel), F_i is the proportion of fraction *i* on the bed surface, u^* is the shear velocity, $\Delta = (\rho_s - \rho_w)/\rho_w$ is the relative submerged density, where ρ_s and ρ_w are the sediment and water densities, respectively, g is the acceleration of gravity, q^*_{bi} is the dimensionless bed load transport rate, ϕ_i is the excess Shields stress (defined below), and A', χ, and ϕ' are parameters for matching the two parts of the q^*_{bi} equation for ϕ_i larger and smaller than φ', respectively. The following equations define the ϕ_i value:

$$\begin{aligned} \phi_i &= \vartheta_i / \vartheta_{ri} \\ \vartheta_i &= \tau / (\Delta \rho_w g d_i) \\ \vartheta_{ri} &= \vartheta_{ri1} + (\vartheta_{ri0} - \vartheta_{ri1})\, e^{-14F_s} \\ \vartheta_{rg0} &= 0.035;\ \vartheta_{rg1} = 0.011;\ \vartheta_{rs1} = 0.065 \\ \vartheta_{rs0} &= \alpha_c \vartheta_{rg0}\left(\frac{dg}{ds}\right) \end{aligned} \tag{A2}$$

where ϑ_i and ϑ_{ri} are the applied and reference Shields numbers, respectively. ϑ_i is defined in terms of the applied shear stress, τ, and the diameter of the *i*th size class. The reference Shields number varies with sediment size (gravel or sand) and with the proportion of sand on the bed, F_s: ϑ_{rg0}, ϑ_{rg1}, ϑ_{rs0}, and ϑ_{rs1} are, respectively, the reference Shields numbers for the gravel size class when $F_s = 0$, the gravel class when $F_s = 1$, the sand class for $F_s = 0$, and the sand class when $F_s = 1$. In the ϑ_{rs0} equation, the parameter α_c is set equal to 1 (Wilcock and Kenworthy, 2002) and dg and ds are representative diameters for the gravel and sand classes, respectively.

Appendix 2

The Einstein–Keulegan resistance equation has the following form:

$$\frac{U}{\sqrt{g\,h'S}} = 2.5\ln\left(\frac{11\,h'}{k_s}\right) \tag{A3}$$

where U is the mean stream velocity, g is the acceleration of gravity, S is the reach slope, k_s is the grain-scale streambed roughness and h' is the effective depth at the reach scale, which is used to define the shear stress acting on the bed $\tau = \rho_w\, g\, h'\, S$, where ρ_w is the water density.

References

Bagnold RA. 1966. The shearing and dilatation of dry sand and the 'singing' mechanism. *Proceedings of the Royal Society of London. Series A: Mathematical and Physical Sciences* **295**(1442): 219–232.

Barry JJ, Buffington JM, King JG. 2004. A general power equation for predicting bedload transport rates in gravel bed rivers. *Water Resources Research* **40**: W10401.

Barnett T, Malone R, Pennell W, Stammer D, Semtner B, Washington W. 2004. The effects of climate change on water resources in the west: introduction and overview. *Climatic Change* **62**: 1–11.

Barton GJ, McDonald RR, Nelson JM, Dinehart RL. 2005. Simulation of Flow and Sediment Mobility Using a Multidimensional Flow Model for the White Sturgeon Critical-habitat Reach, Kootenai River Near Bonners Ferry, Idaho. US Geological Survey Scientific Investigations Report 2005–5230. US Geological Survey: Reston, VA.

Bisson PA, Rieman BE, Luce C, Hessburg PF, Lee DC, Kershner JL, Reeves GH, Gresswell RE. 2003. Fire and aquatic ecosystems of the western USA: current knowledge and key questions. *Forest Ecology and Management* **178**(1–2): 213–229.

Bjornn TC, Reiser DW. 1991. Habitat requirements of salmonids in streams. In *Influence of Forest and Rangeland Management on Salmonid Fishes and their Habitats*, Meehan WR (ed). American Fisheries Society Special Publication 19: Bethesda, MD; 83–138.

Bjornn TC, Brusven MA, Molnau MP, Milligan JH, Klant RA, Chaco E, Shaye C. 1977. Transport of granitic sediment in streams and its effects on insects and fish. Forest, Wildlife and Range Experiment Station Bulletin 17. University of Idaho: Moscow, ID; 43.

Buffington JM, Montgomery DR, Greenberg HM. 2004. Basin-scale availability of salmonid spawning gravel as influenced by channel type and hydraulic roughness in mountain catchments, *Canadian Journal of Fisheries and Aquatic Sciences* **61**(11): 2085–2096.

Burner CJ. 1951. Characteristics of spawning nests of Columbia River salmon. *US Fish and Wildlife Service Bulletin* **61**: 97–110.

Cannon SH, Gartner JE, Rupert MG, Michael JA, Rea AH, Parrett C. 2010. Predicting the probability and volume of post-wildfire debris flows in the intermountain western United States. *Geological Society of America Bulletin* **122**: 127–144.

Cao Z, Carling PA. 2003. On evolution of bed material waves in alluvial rivers. *Earth Surface Processes and Landforms* **28**(4): 437–441.

Chapman DW. 1988. Critical review of variables used to define effects of fines in redds of large salmonids. *Transactions of the American Fisheries Society* **117**(1): 1–21.

Cheng N-S, Chiew Y-M. 1999. Analysis of initiation of sediment suspension from bed load. *Journal of Hydraulic Engineering* **128**(8): 232–235.

Cover MR, May CL, Dietrich WE, Resh VH. 2008. Quantitative linkages among sediment supply, streambed fine sediment, and benthic macroinvertebrates in northern California streams. *Journal of the North American Benthological Society* **27**(1): 135–149.

Cui Y, Parker G. 2005. Numerical model of sediment pulses and sediment-supply disturbances in mountain rivers. *Journal of Hydraulic Engineering* **131**(8): 646–656.

Cui Y, Parker G, Lisle TE, Gott J, Hansler-Ball ME, Pizzuto JE, Allmendinger NE, Reed JM. 2003a. Sediment pulses in mountain rivers: 1. Experiments. *Water Resources Research* **39**(9): WR001803.

Cui Y, Parker G, Pizzuto J, Lisle TE. 2003b. Sediment pulses in mountain rivers: 2. Comparison between experiments and numercial predictions. *Water Resources Research* **39**(9): WR001805.

Cummins KW, Lauff GH. 1969. The influence of substrate particle size on the microdistribution of stream macrobenthos. *Hydrobiologia* **34**(2): 145–181.

Dietrich WE. 1982. Settling velocity of natural particles. *Water Resources Research* **18**(6): 1615–1626.

Dietrich WE, Smith JD. 1983. Influence of the point bar on flow through curved channels. *Water Resources Research* **19**(5): 1173–1192.

Dietrich WE, Smith JD. 1984. Bed load transport in a river meander. *Water Resources Research* **20**(10): 1355–1380.

Everest FH, Beschta RL, Scrivener JC, Koski KV, Sedel JR, Cederhom CJ. 1987. Fine sediment and salmonid production a paradox. In *Streamside Management: Forestry and Fishery Interaction*, Salo EO, Cundy TW (eds). Institute of Forest Resources: University of Washington, Seattle; 143–190.

Gomez B, Church M. 1989. An assessment of bed load sediment transport formulae for gravel bed rivers. *Water Resources Research* **25**(6): 1161–1186.

Goode JR, Luce CH, Buffington JM. 2012. Enhanced sediment delivery in a changing climate in semi-arid mountain basins: implications for water resource management and aquatic habitat in the northern Rocky Mountains. *Geomorphology* **139–140**: 1–15. doi:10.1016/j.geomorph.2011.06.021.

Goode JR, Buffington JM, Tonina D, Isaak DJ, Thurow RF, Wenger S, Nagel D, Luce CH, Tetzlaff D, Soulsby C. 2013. Potential effects of climate change on streambed scour and risks to salmonid survival in snow-dominated mountain basins. *Hydrological Processes* **27**: 750–765. doi:10.1002/hyp.9728.

Grams PE, Schmidt JC, Andersen ME. 2010. High-flow experiment at Glen Canyon Dam - morphologic response of eddy-deposited sandbars and associated aquatic backwater habitats along the Colorado River in Grand Canyon National Park, US Geological Survey Open-File Report 2010–1032.

Grieg SM, Sear AD, Carling PA. 2005. The impact of fine sediment accumulation on the survival of incubating salmon progeny: implications for sediment managment. *Science of the Total Environment* **344**(1–3): 241–258.

Hansler ME. 1999. Sediment wave evolution and analysis of a one-dimensional sediment routing model, Navarro River, Northwestern California. MS thesis. Humboldt State University, Arcata, CA.

Hoffman DF, Gabet EJ. 2006. Effects of sediment pulses on channel morphology in a gravel-bed river. *Geological Society of America Bulletin* **119**(1–2): 116–125. doi: 10.1130/B25982.1.

Humphries R, Venditti JG, Sklar LS, Wooster JK. 2012. Experimental evidence for the effect of hydrographs on sediment pulse dynamics in gravel-bedded rivers. *Water Resources Research* **48**: W01533. doi: 10.1029/2011WR010419.

Isaak DJ, Thurow RF. 2006. Network-scale spatial and temporal variation in Chinook salmon (*Oncorhynchus tschawytscha*) redd distributions: patterns inferred from spatially continuous replicate surveys. *Canadian Journal of Fisheries and Aquatic Sciences* **63**(2): 285–296.

Istanbulluoglu ED, Tarboton G, Pack RT, Luce C. 2002. A probabilistic approach for channel initiation. *Water Resources Research* **38**(12): 1325. doi: 10.1029/2001 WR000782.

Istanbulluoglu ED, Tarboton DG, Pack RT, Luce CH. 2004. Modeling of the interactions between forest vegetation, disturbances, and sediment yields. *Journal of Geophysical Research - Earth Surface* **109**: F01009.

King JG, Emmett WW, Whiting PJ, Kenworthy RP, Barry JJ. 2004. Sediment Transport Data and Related Information for Selected Gravel-bed Streams and Rivers in Idaho. US Forest Service General Technical Report RMRS-GTR-131. USDA Forest Service, Rocky Mountain Research Station: Fort Collins, CO.

Langbein WB, Leopold LB. 1968. River channel bars and dunes - theory of kinematic waves. US Geological Survey Professional Paper 422-L; US Government Printing Office, Washington, DC.

Lapointe MF, Bergeron NE, Bérubé F, Pouliot M-A, Johnston P. 2004. Interactive effects of substrate sand and silt contents, redd-scale hydraulic gradients, and interstitial velocities on egg-to-emergence survival of Atlantic salmon (*Salmo salar*). *Canadian Journal of Fisheries and Aquatic Sciences* **61**(12): 2271–2277.

Lisle TE, Pizzuto JE, Ikeda H, Iseya F, Kodama Y. 1997. Evolution of a sediment wave in a experimental channel. *Water Resources Research* **33**(8): 1971–1981.

Lisle TE, Cui Y, Parker G, Pizzuto JE, Dood AM. 2001. The dominance of dispersion in the evolution of bed material waves in gravel-bed rivers. *Earth Surface Processes and Landforms* **26**(13): 1409–1420.

Long CE, Wiberg PL, Nowell ARM. 1993. Evaluation of von Karman's constant from integral flow parameters. *Journal of Hydraulic Engineering* **119**: 1182–1190.

May CL, Pryor B, Lisle TE, Lang M. 2009. Coupling hydrodynamic modeling and empirical measures of bed mobility to predict the risk of scour and fill of salmon redds in a large regulated river. *Water Resources Research* **45**: W05402.

McDonald RR, Bennett JP, Nelson JM. 2001. The USGS multi-dimensional surface water modeling system. In *Proceedings of the 7th Interagency Sedimentation Conference*, March 25–29 2001. US Geological Survey: Reno, NV; I-161–I-167.

McDonald RR, Nelson JM, Bennett JP. 2005. Multi-Dimensional Surface-Water Modeling System User's Guide. US Geological Survey Techniques and Methods 6-B2. US Geological Survey; Reston, VA.

McKean J, Isaak D, Wright CW. 2009a. Stream and riparian habitat analysis and monitoring with a high-resolution terrestrial-aquatic lidar. In *PNAMP Special Publication: Remote Sensing Applications for Aquatic Resource Monitoring*, Bayer JM, Schei JL (eds). Pacific Northwest Aquatic Monitoring Partnership: Cook, Washington; 7–16.

McKean J, Nagel D, Tonina D, Bailey P, Wright CW, Bohn C, Nayegandhi A. 2009b. Remote sensing of channels and riparian zones with a narrow-beam aquatic-terrestrial lidar. *Remote Sensing* **1**(4): 1065–1096.

McKean JA, Tonina D. 2013. Bed stability in unconfined gravel-bed mountain streams: With implications for salmon spawning viability in future climates. *Journal of Geophysical Research - Earth Surface* **118**: 1–14. doi:10.1002/jgrf.20092.

Megahan WF, Platts W, Kulesza B. 1980. *Riverbed improves over time: South Fork Salmon. Symposium on Watershed Management*. American Society of Civil Engineers: New York; 380–395.

Miller D, Luce C, Benda L. 2003. Time, space, and episodicity of physical disturbance in streams. *Forest Ecology and Management* **178**: 121–140.

Moody JA, Martin DA. 2009. Synthesis of sediment yields after wildland fire in different rainfall regimes in the western United States. *International Journal of Wildland Fire* **18**: 96–115.

Mote PW, Hamlet AF, Clark MP, Letternmaier DP. 2005. Declining mountain snow pack in western North America. *Bulletin of the American Meteorological Society* **86**: 39–49.

Nelson JM, McDonald RR. 1997. Mechanics and modeling of flow and bed evolution in lateral separation eddies. Glen Canyon Enviromental Report. 69.

Nelson JM, Bennett JP, Wiele SM. 2003. Flow and sediment transport modeling. In *Tools in Geomorphology*, Kondolph GM, Piegay H (eds). John Wiley & Sons: Chichester; 539–576.

Nelson J, McDonald RR, Kinzel P. 2006. Morphologic evolution in the USGS surface-water modelling system. In *Proceeding of the 8th Federal Interagency Sedimentation Conference*, Reno, NV, April 2–6 2006. US Geological Survey: Reno; 233–240.

Reeves GH, Benda LE, Burnett KM, Bisson PA, Sedell JR. 1995. A disturbance-based ecosystem approach to maintaining and restoring freshwater habitats of evolutionarily significant units of anadromous salmonids in the Pacific Northwest. In *Evolution and the Aquatic Ecosystem: Defining Unique Units in Population Conservation*, Nielsen JL (ed). American Fisheries Society Symposium 17: Bethsda, MD; 334–349.

Rhodes JJ, McCullough DA, Espinosa FAJ. 1994. A coarse screeening process for evaluation of effects of land management activities on salmon spawning and rearing habitat in ESA consultations. Columbia River Inter-Tribal Fish Commission, Portland, OR.

Rieman BE, Lee DC, Chandler G, Myers D. 1997. Does wildfire threaten extinction for salmonids? Responses of redband trout and bull trout following recent large fires on the Boise National Forest. In *Proceedings of the Conference on Wildfire and Threatened and Endangered Species and Habitats*, Greenlee J (ed). International Association of Wildland Fire: Fairfield, WA; 47–57.

Rieman BE, Lee D, Burns D, Gresswell R, Young M, Stowell R, Rinne J, Howell P. 2003. Status of native fishes in the western United States and issues for fire and fuels management. *Forest Ecology and Management* **178**: 197–211.

Riemann L, Farnelid H, Steward GF. 2010. Nitrogenase genes in non-cyanobacterial plankton: prevalence, diversity and regulation in marine waters. *Aquatic Microbiological Ecology* **61**: 235–247.

Rubin DM, Topping DJ. 2001. Quantifying the relative importance of flow regulation and grain size regulation of suspended sediment transport α and tracking changes in grain size of bed sediment β. *Water Resources Research* **37**(1): 133–146.

Shakesby RA, Doerr SH. 2006. Wildfire as a hydrological and geomorphological agent. *Earth - Science Reviews* **74**(3–4): 269–307.

Sklar LS, Fadde J, Venditti JG, Nelson P, Wydzga MA, Cui Y, Dietrich WE. 2009. Translation and dispersion of sediment pulses in flume experiments simulating gravel augmentation below dams. *Water Resources Research* **45**: W08439. doi: 10.1029/2008WR007346.

Suttle KB, Power ME, Levine JB, McNeely C. 2004. How fine sediment in riverbeds impairs growth and survival of juvenile salmonids. *Ecological Applications* **14**(4): 969–974.

Tonina D, Buffington JM. 2009. A three-dimensional model for analyzing the effects of salmon redds on hyporheic exchange and egg pocket habitat. *Canadian Journal of Fisheries and Aquatic Sciences* **66**(12): 2157–2173.

Tonina D, Jorde K. 2013. Hydraulic modeling approaches for ecohydraulic studies: 3D, 2D, 1D and non-numerical models. In *Ecohydraulics: An Integrated Approach*, Maddock I, Harby A, Kemp P, Wood P (eds). Wiley-Blackwell: New Delhi, India, 31–66.

Tonina D, McKean JA. 2010. Climate change impact on salmonid spawning in low-gradient streams in central Idaho, USA. In *Proceeding of the 9th International Conference on Hydroinformatics Tiajin. China*, Tao J, Cheng Q, Liong S-Y (eds). September 7–11, Chemistry Industry Press: Beijing; 389–397.

Tonina D, McKean JA, Buffington JM, Luce C, Dietrich WE. 2007. Numerical model to analyze the effects of sediment supply on river morphology and streambed characteristics. *EOS AGU Transactions* **88**: H53L-06.

Wiberg PL, Smith JD. 1991. Velocity distribution and bed roughness in high-gradient streams. *Water Resources Research* **27**(5): 825–838.

Whiting PJ, Dietrich WE. 1990. Boundary shear stress and roughness over mobile alluvial beds. *Journal of Hydraulic Engineering* **116**(12): 1495–1511.

Wilcock PR, Kenworthy ST. 2002. A two-fraction model for the transport of sand/gravel mixtures. *Water Resources Research* **38**(10): WR000684.

Wolman MG. 1954. A method of sampling coarse bed material. *Transactions American Geophysical Union* **35**: 951–956.

Wood PJ, Armitage PD. 1997. Biological effects of fine sediment in the lotic environment. *Environmental Management* **21**(2): 203–217.

Wu F-C. 2000. Modeling embryo survival affected by sediment deposition into salmonid spawning gravels: application to flushing flow prescriptions. *Water Resources Research* **36**(6): 1595–1603.

Wu F-C, Chou Y-J. 2003. Simulation of gravel-sand bed response to flushing flows using a two-fraction entrainment approach: model development and flume experiment. *Water Resources Research* **39**(8): WR001284.

Yount JD, Niemi GJ. 1990. Recovery of lotic communities and ecosystems from disturbance - a narrative review of case studies. *Environmental Management* **14**: 547–570.

